

# Design, Synthesis, and Characterization of Novel Small Molecules as Broad Range Antischistosomal Agents

Anastasia Rugel,<sup>‡,○</sup> Reid S. Tarpley,<sup>†,○</sup> Ambrosio Lopez,<sup>†</sup> Travis Menard,<sup>†</sup> Meghan A. Guzman,<sup>‡</sup> Alexander B. Taylor,<sup>§,⊥</sup> Xiaohang Cao,<sup>§</sup> Dmytro Kovalsky,<sup>||</sup> Frédéric D. Chevalier,<sup>#</sup> Timothy J. C. Anderson,<sup>#</sup> P. John Hart,<sup>§,⊥,▽</sup> Philip T. LoVerde,<sup>\*,‡</sup> and Stanton F. McHardy<sup>\*,†,⊥</sup>

<sup>†</sup>Center for Innovative Drug Discovery, University of Texas at San Antonio, Department of Chemistry, One UTSA Circle, San Antonio, Texas 78249, United States

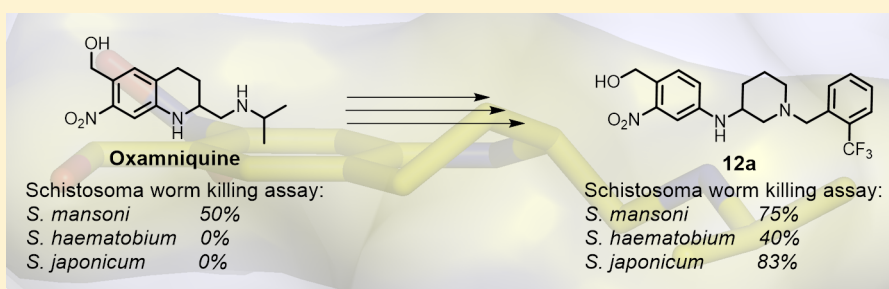
<sup>‡</sup>Department of Pathology and Laboratory Medicine, <sup>§</sup>Department of Biochemistry and Structural Biology, and <sup>||</sup>Greehey Children's Cancer Research Institute, UT Health San Antonio, 7703 Floyd Curl Drive, San Antonio, Texas 78229, United States

<sup>⊥</sup>X-ray Crystallography Core Laboratory, Institutional Research Cores, UT Health San Antonio, 7703 Floyd Curl Drive, San Antonio, Texas 78229, United States

<sup>#</sup>Texas BioMedical Research Institute, 7620 NW Loop 410, San Antonio, Texas 78227-5301, United States

<sup>▽</sup>Department of Veterans Affairs, South Texas Veterans Health Care System, San Antonio, Texas 78229, United States

## Supporting Information



**ABSTRACT:** Schistosomiasis is a major human parasitic disease afflicting more than 250 million people, historically treated with chemotherapies praziquantel or oxamniquine. Since oxamniquine is species-specific, killing *Schistosoma mansoni* but not other schistosome species (*S. haematobium* or *S. japonicum*) and evidence for drug resistant strains is growing, research efforts have focused on identifying novel approaches. Guided by data from X-ray crystallographic studies and *Schistosoma* worm killing assays on oxamniquine, our structure-based drug design approach produced a robust structure–activity relationship (SAR) program that identified several new lead compounds with effective worm killing. These studies culminated in the discovery of compound **12a**, which demonstrated broad-species activity in killing *S. mansoni* (75%), *S. haematobium* (40%), and *S. japonicum* (83%).

**KEYWORDS:** Schistosomiasis, oxamniquine, structure–activity relationships, X-ray crystallographic studies, aminopyrrolidine, aminopiperidine

Schistosomiasis is a neglected tropical disease caused by flatworms of the genus *Schistosoma*. After malaria, it is the second most endemic parasitic disease, estimated to affect over 250 million people worldwide and is responsible for almost 200,000 deaths each year.<sup>1</sup> There are three major pathogenic species of *Schistosoma*: *S. haematobium* (Africa, 119 million cases), *S. mansoni*, (South America and Africa, 67 million cases), and *S. japonicum* (South-East Asia, 1 million cases). Although some small therapeutics have been employed (Figure 1) to combat the disease, broad range efficacy and effectiveness to drug-resistant strains of *Schistosoma* still represent a significant unmet medical need.<sup>2</sup> The general antiparasitic drug Praziquantel **1** is the only treatment on the market and is active against all species of *Schistosoma*. Oxamniquine **3** was discovered through an

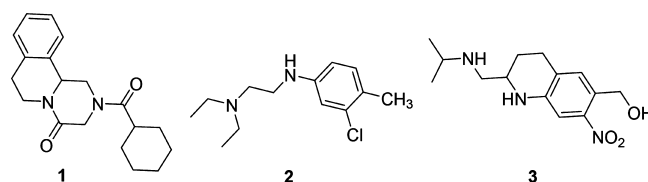


**Figure 1.** Structure of Praziquantel **1**, Mirasan **2**, and Oxamniquine **3**. The hydroxymethyl moiety of **3** is sulfated by SmSULT-OR.

**Received:** June 3, 2018

**Accepted:** September 14, 2018

**Published:** September 14, 2018

optimization study on Mirasan **2**, a lead found by Kikuth and Gönner at Bayer. Compound **2** was found to have schistosomidal activity in mice while completely inactive in a monkey model. It was later discovered that an active metabolite isolated from the urine of treated mice proved to have high potency on other species. The Mirasan series was revived at Pfizer in 1968, in which they found that an active metabolite, the hydroxymethyl derivative of **2**, UK-3883, was three times as potent as **2**. Through structure–activity relationships (SARs) and lead optimization, **3** was developed and used as first-line treatment in Brazil until the late 1990s and remained in use until 2010.<sup>3</sup> It has a robust safety record, but unlike **1**, its treatment efficacy is limited to *S. mansoni*.<sup>4</sup>

In 2013, Valentim et al. discovered the mechanism of action of **3** by a genetic approach and comparison of gene sequences of oxamniquine-sensitive and resistant *S. mansoni*. Compound **3** is a prodrug, which, through sulfation of the hydroxymethyl moiety (Figure 1), is converted to the active species upon exposure to a sulfotransferase present in *S. mansoni* (SmSULT-OR). The active drug is then released from the enzyme and alkylates the parasite's DNA [in a  $S_N2$  reaction] resulting in the death of the parasite.<sup>5,6</sup> In order to understand the molecular basis of resistance, SmSULT-OR was cocrystallized with **3** and the sulfate-depleted version of its cofactor, 3'-phosphoadenosine 5'-phosphonate (PAP). From these X-ray structures shown in Figure 2, it was determined that **3**

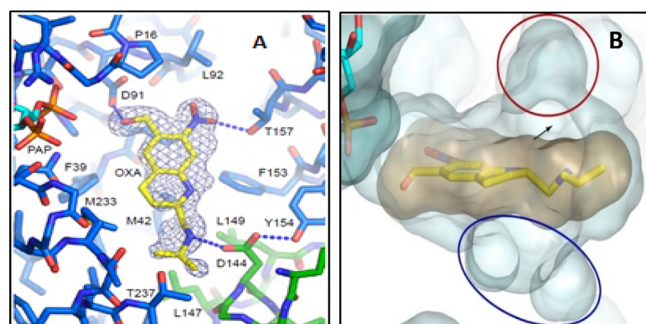


**Figure 2.** (A) Oxamniquine **3** bound to SmSULT-OR with key contacts. (B) Lipophilic pockets (blue and red) above and below OXA structure.

makes 98 contacts with the central cavity of SmSULT-OR, with the most important interactions being van der Waals interactions with F39, F153, and M233 as well as three hydrogen bonds with D91, T157, and D144. Specifically, D91 forms an H-bond with the benzyl alcohol, T157 with the nitro group, and D144 with N12. As shown in Figure 2B, lipophilic pockets above and below the central binding cavity of **3** were identified. Additionally, phylogenetic analysis found homologous sulfotransferases for *S. haematobium* and *S. japonicum* with SmSULT-OR.

Despite significant sequence identity shared between SmSULT-OR and the sulfotransferases in *S. haematobium* (71%) and *S. japonicum* (58%), **3** is effective only against *S. mansoni*. Alignment of the crystal structures indicates that the three enzymes have the same catalytic mechanism, but sequence variations in the active site such as a phenylalanine in SmSULT-OR (F39) to tyrosine in the others and a glycine in SmSULT-OR (G143) to valine in *S. japonicum* were predicted to negatively impact compound **3**'s binding and efficacy for the resistant species.<sup>5,6</sup> Using a genetic, molecular biology, and biochemistry approach, we demonstrated that a schistosome sulfotransferase was responsible for the mode of action of oxamniquine.<sup>5</sup> Comparison of the DNA sequence of the sulfotransferase from a susceptible worm with the sequence from a resistant worm

identified the deletion of a glutamate at position 142 as responsible for drug resistance. This was confirmed by a functional assay and in the crystal structure of the sulfotransferase,<sup>5</sup> which showed that deletion of glutamate 142 would likely disrupt an  $\alpha$ -helix containing aspartate 144 that forms a hydrogen bond to oxamniquine. Current treatment for schistosomiasis uses a praziquantel monotherapy, and a recent review article provides evidence for schistosomes with decreased praziquantel sensitivity in the field in Africa.<sup>7</sup> Thus, a structure-based design strategy (Figure 3) of oxamniquine derivatives, to be used alongside

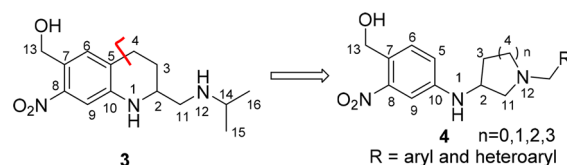


**Figure 3.** Design of novel analog subtype **4**.

praziquantel as a combination therapy, could possibly surmount developing praziquantel resistance as the two drugs act on different targets.

To date, the development of novel antischistosomal agents has focused on a variety of small molecule approaches,<sup>8,9</sup> including statins,<sup>10</sup> cysteine proteases,<sup>11</sup> anticancer and kinase targets,<sup>12–14</sup> and natural products,<sup>15</sup> as examples. Additional analog design approaches have focused on FDA registered drugs, such as **1** or **3**, as either starting points for further derivatization and/or as the basis for SAR studies.<sup>16–21</sup> More recently, ruthenocenyl- and ferrocenyl-based organometallic oxamniquine conjugates have also been described.<sup>22</sup> Given the high production costs and diminishing supply of oxamniquine, partially due to a biotransformation hydroxylation process,<sup>23,24</sup> our approach focused on developing a novel small molecule that had efficacious broad-range antischistosomal activity and favorable “drug-like” physicochemical properties and ultimately provided an opportunity for a simplified and efficient synthesis approach. Thus, the goal of our research program was to initiate a structure-based drug design approach based on the X-ray structural data of SmSULT-OR and compound **3**, as well as the structural information on *S. haematobium* and *S. japonicum* to identify a novel small molecule that would be capable of effective killing activity across all three species of *Schistosoma* and show activity against **1** resistant forms. Herein we report the design, synthesis, and *in vitro* evaluation of novel analogs of compound **3**, lead compounds of which have been shown to be efficacious against all three species of *Schistosoma*.

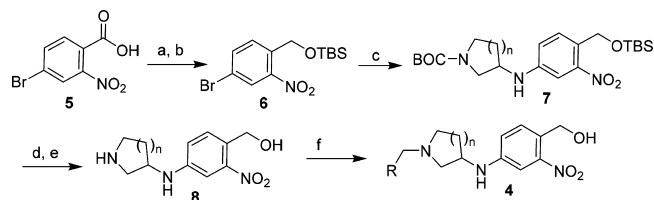
To identify novel, broad-acting antischistosomal agents of general structure **4**, we envisioned structural modifications to **3** to accomplish the following (Figure 3): (1) maintain the required 4-amino-2-nitro-benzyl alcohol moiety based on the pro-drug sulfotransferase mechanism associated with compound **3**, (2) remove an element of rigidity by removing the tetrahydroquinoline ring of **3** and introduce two rotatable bonds between C10–N1 and N1–C2, (3) install various heterocyclic rings between C2 to N12 to explore the structural effects of different ring sizes, and (4) introduce lipophilic groups (R = aryl and heteroaryl) off of the N12 position to possibly access the lipophilic regions highlighted above in Figure 2B.

In addition to these structure-based drug design objectives, we also incorporated *in silico* drug-like physicochemical property calculations and *in silico* molecular modeling and docking studies to aid in compound design cycles. Thus, we aimed to maintain

favorable “drug-like” physicochemical properties (LogP, tPSA, MW, and number of hydrogen bond donors/acceptors) across all analogs to maintain good solubility and ADME properties.<sup>25,26</sup>

The analogs prepared for these studies were synthesized as highlighted in Scheme 1. This synthesis strategy was designed to

### Scheme 1. General Synthesis Route To Prepare Compound 4<sup>a</sup>



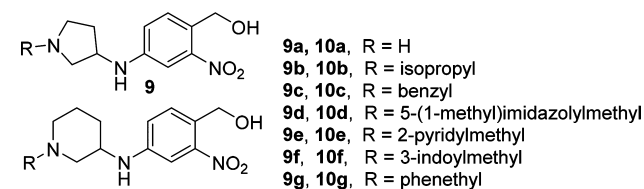
<sup>a</sup>Reagents and conditions: (a)  $\text{BH}_3$ , THF, THF, 93%; (b) TBSCl, imidazole, DCM, 81%; (c)  $\text{Pd}(\text{OAc})_2$ , BINAP,  $\text{Cs}_2\text{CO}_3$ , 1,4-dioxane, N-Boc-heterocyclic amine, 50–80%; (d) TBAF, THF, 90–98%; (e)  $\text{BF}_3\text{OEt}_2$ , DCM,  $-10^\circ\text{C}$  to r.t., 1 h, 71–99%; (f)  $\text{NaBH}(\text{OAc})_3$ , 1,2-DCE, r.t., RCHO, 50–90%.

accomplish two goals: (1) to have flexibility to incorporate numerous N-Boc-cyclic amine templates for structural diversity and (2) to allow for late-stage diversification of the R groups through reductive amination, both of which would support evaluation and SAR development across numerous analogs. Starting from commercially available 4-bromo-2-nitrobenzoic acid **5**, reduction with  $\text{BH}_3$ -THF<sup>27</sup> followed by protection of the resulting alcohol as a TBS ether produced the desired compound **6**.<sup>28</sup> Compound **6** was then used as a common intermediate for Buchwald–Hartwig amination conditions<sup>29,30</sup> with a variety of commercially available N-Boc-protected diamines, producing a diverse set of cyclic amine templates (compound **7**) in moderate to good yields (50–80%).

Simultaneous deprotection of the N-Boc and TBS-ether groups in compound **7** under a variety of conditions screened proved to be problematic and produce complex product mixtures. Thus, a two-step deprotection sequence utilizing TBAF-mediated removal of the TBS group (90–98%), followed by  $\text{BF}_3\text{OEt}_2$  deprotection of the N-Boc group<sup>31</sup> was employed. This two-step transformation cleanly produced the desired amine **8**, which was then further functionalized via reductive amination conditions with various aldehydes to produce the final analogs (template **4**) for screening. All analogs were prepared as racemic mixtures.

In order to test our central hypothesis in our design strategy, our first research objective was to explore the effects of various heterocyclic ring cores and a small number of different R-groups had on *S. mansoni*. Table 1 highlights our initial investigations focused on the 3-aminopyrrolidine (compounds **9a**–**9g**) and 3-aminopiperidine (compounds **10a**–**10g**) templates. We were encouraged with the initial result showing the secondary amine derivative of the 3-aminopiperidine core, compound **10a**, displayed moderate activity (50%) in killing *S. mansoni*. Interestingly, the corresponding structural analog in the 3-aminopyrrolidine series (compound **9a**) was found to be significantly less active than **3** or **10a**. These initial results prompted us to prepare a number of analogs with substitution on the nitrogen atoms of the piperidine and pyrrolidine rings. Small alkyl side chains (isopropyl) showed a decrease in *S. mansoni* killing activity relative to compound **3**, as highlighted by analogs **9b** and **10b**. Increasing the size and aromatic nature of the R-group produced some interesting results. Benzyl groups showed a marked increase in *S. mansoni* killing activity for both series as

Table 1. SAR Data on Worm Killing of *S. mansoni*.



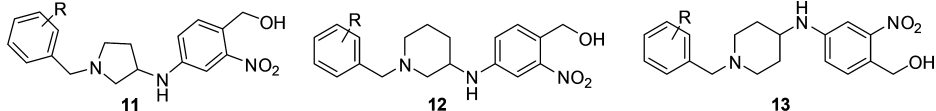
Entry	<sup>a</sup> % Killing ( <i>S. m.</i> )	Entry	<sup>a</sup> % Killing ( <i>S. m.</i> )
9a	10	10a	50
9b	40	10b	10
9c	75 ± 15	10c	60
9d	0	10d	20
9e	0	10e	0
9f	85 ± 15	10f	26
9g	7	10g	40

<sup>a</sup>Compounds were tested against adult male *S. mansoni* (*S. m.*) worms in vitro. All compounds were tested at a final concentration of 143  $\mu\text{M}$ . Percent killing value and sd are reported. All screens were performed in experimental and biological triplicate. Positive control, compound **3** kills 85% ± 15 of *S. mansoni* parasites in vitro.

observed with compounds **9c** and **10c**. Additionally, heterocyclic groups such as pyridines or imidazolyl (**9d**–**e** and **10d**–**e**) were not well tolerated for either core; however, the 3-indolylmethyl substitution on the 3-aminopyrrolidine core (compound **9f**) showed equivalent activity to **3**. Finally, as a direct comparison to the secondary piperidine amine **10a**, increasing the size of the heterocyclic ring to an azepane or decreasing the size of the ring to the corresponding azetidines significantly decreased the activity in killing *S. mansoni* (see SI Table S1). Increasing the length of the R group to phenethyl also showed a decrease in activity (**9g** and **10g**).

Following these results, we expanded our investigations to include 4-aminopiperidines derivatives as well as the 3-aminopiperidines and 3-aminopyrrolidine cores. We explored the effects of benzyl substitution across all three series, testing for activity on *S. mansoni*. As highlighted in Table 2, across the series, benzyl derivatives substituted with certain polar groups (i.e.,  $-\text{NO}_2$ ,  $-\text{CN}$ ,  $-\text{OCH}_3$ ) or halogens in the 2- or 4-position showed a marked decrease across all three templates when compared to the unsubstituted benzyl derivatives (**9c** and **10c**). However, 2-trifluoromethyl (**12a**), 3-trifluoromethyl (**11h** and **12d**), 2-trifluoromethoxy (**11d**), and 4-trifluoromethoxy (**11g**) derivatives were shown to exhibit high activity against *S. mansoni* depending on the specific amine core. The trend appears to show preference for lipophilic moieties, which is consistent with the tyrosine and phenylalanine residues occupying the binding pocket for this side chain. To test the limits of these trends, bis-2,4-trifluoromethyl, 2-methyl, and 4-*tert*-butyl substitutions of the 3-aminopiperidine core were prepared; however, they failed to exhibit any substantial killing activity for *S. mansoni* (see SI Table S1).

Based on the SAR results above, compounds **9f**, **11d**, **11f**, **11h**, **12a**–**12d**, and **13b**–**13c** were screened against *S. haematobium* and if active, *S. japonicum* (Table 2). Compound **3** is completely inactive against *S. haematobium* and *S. japonicum*. The 3-aminopyrrolidine analogs **9f**, **11f**, and **11h** showed no appreciable activity against *S. haematobium*, while the corresponding *p*- $\text{OCF}_3$  analog, **11g**, showed modest activity. Unfortunately, **11g** was inactive against *S. japonicum*, and the 2- $\text{OCF}_3$  derivative **11d** was inactive against *S. haematobium*. In the 3-aminopiperidine series,

Table 2. SAR Data on Worm Killing of *S. mansoni* (*S. m.*), *S. haematobium* (*S. h.*), and *S. japonicum* (*S. j.*)<sup>a</sup>


3-aminopyrrolidines (11)					3-aminopiperidines (12)				
Entry	R=	% Killing ( <i>S. m.</i> )	% Killing ( <i>S. h.</i> )	% Killing ( <i>S. j.</i> )	Entry	R=	% Killing ( <i>S. m.</i> )	% Killing ( <i>S. h.</i> )	% Killing ( <i>S. j.</i> )
11a	2-OMe	7	ND	ND	12a	2-CF <sub>3</sub>	75 ± 5	40	83
11b	2-F	30	ND	ND	12b	2-OCF <sub>3</sub>	84	<40	ND
11c	2-CF <sub>3</sub>	27	ND	ND	12c	4-OCF <sub>3</sub>	40	43	10
11d	2-OCF <sub>3</sub>	100	<40	ND	12d	3-CF <sub>3</sub>	100	2	2
11e	4-NO <sub>2</sub>	17	ND	ND	4-aminopiperidines (13)				
11f	4-CF <sub>3</sub>	100	10	ND	Entry	R=	% Killing ( <i>S. m.</i> )	% Killing ( <i>S. h.</i> )	% Killing ( <i>S. j.</i> )
11g	4-OCF <sub>3</sub>	87	40	0	13a	2-CF <sub>3</sub>	20	ND	ND
11h	3-CF <sub>3</sub>	93	8	ND	13b	4-CF <sub>3</sub>	81 ± 11	0	ND
11i	3-OCF <sub>3</sub>	60	ND	ND	13c	4-OCF <sub>3</sub>	97	14	ND
11j	2,4-diCl	17	ND	ND					

<sup>a</sup>Percent killing value is reported for *S. mansoni*, *S. haematobium*, and *S. japonicum* worms in vitro. All derivatives were solubilized in 100% DMSO and administered at a final concentration of 143 μM per well for all assays. All screens were performed in experimental and biological triplicate. Positive control, compound 3 kills 85% ± 15 of *S. mansoni* parasites in vitro. ND, not determined.

12a and 12c showed promising activity against *S. haematobium*, and compound 12a was found to kill >80% of *S. japonicum* worms at the end of the 12-day study. The most active 4-aminopiperidine analogs in *S. mansoni* (13b and 13c) were found to be void of any appreciable activity against *S. haematobium*.

The worm killing SAR differences can be influenced by factors outside of direct SmSULT-OR binding interactions, such as kinetics of the sulfotransferase process, membrane permeability, and metabolic stability. However, given the structural and property similarities between the different chemical series investigated, we rationalized some of the differences observed in *S. mansoni* SAR through modeling and docking studies. Docking of all 9–13 compounds from Tables 1 and 2 (both S- and R-enantiomers) provided docking scores partially consistent with the observed SAR in *S. mansoni*, which suggested a preference for the -CF<sub>3</sub> substitution (see Table S3 in SI). A selection of some of the best performing compounds in the docking studies are overlaid in Figure 4 (11f, 12a, 12d, and 13b), suggesting crucial π-π stacking interactions of the phenyl groups with the F39 and F43 residues, while the carboxyl group of D144 forms a salt bridge with the pyrrolidine or piperidine nitrogen. Conversely, some

compounds with para substitution, namely, 11e and 11j have also received similar scores; however, they performed poorly in the *S. mansoni* killing assay. The sequence variations in the active site for *S. haematobium* and *S. japonicum* discussed earlier might cause preferential binding on specific CF<sub>3</sub>-phenyl analogs like 12a; however, docking studies on *S. haematobium* and *S. japonicum* were inconclusive. This discrepancy might be rationalized by limitations of current force field calculations to account for unique properties of fluorine in small molecule–protein interactions, an observed phenomenon with extensive literature precedent;<sup>32</sup> thus, further structural and binding studies are warranted to provide insight into these observed species differences.

Compound 12a (Figure 5) represents an extremely interesting compound for further follow up studies due to the demonstrated

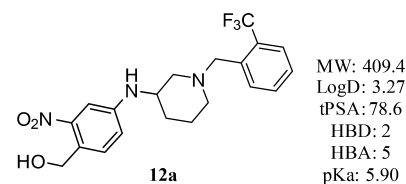


Figure 5. Structure and physicochemical properties of 12a.

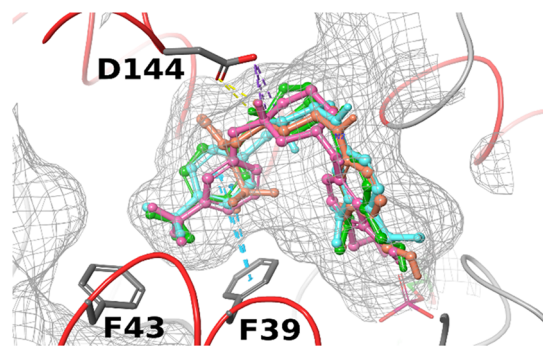
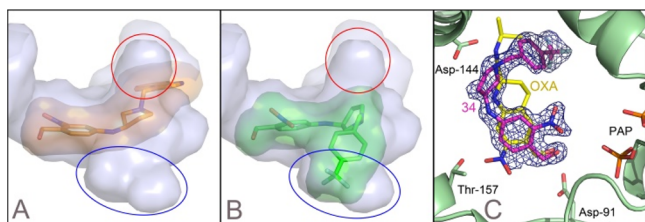


Figure 4. Molecular docking in *S. mansoni*. Superposition of docking poses of high scoring compounds 11f (green), 12a (orange), 12d (pink), and 13b (cyan) in *S. mansoni* suggesting -CF<sub>3</sub> aryl groups bind to side chains of F39 and F43. Protein surface shown in mesh. D144 forms a salt bridge with protonated nitrogen and hydrogen bond with its hydrogen.

broad-species activity in killing (*S. mansoni*, 75%; *S. haematobium*, 40%; and *S. japonicum*, 83%) and favorable drug-like physicochemical properties (Figure 5).<sup>33</sup>

Compound 12a is profiled and reported herein as a racemic mixture; however, preparation of the enantiomers and detailed *in vitro* and *in vivo* characterization will be reported in due course.

Our most active analogs were soaked in racemic form into native *S. mansoni* sulfotransferase crystals containing PAP; however, preferential binding of enantiomers (*R*)-9f and (*S*)-11f was observed.<sup>34</sup> The structures show that compounds were able to enter and bind in the active site without major conformational changes to the unbound enzyme structure. All compounds are observed in the active site overlapping with the oxamniquine position (Figure 6). Interestingly, for compound (*S*)-11f (Figure 6B), the phenyl ring containing the nitro- and hydroxymethyl groups is rotated 180° such that the nitro moiety is



**Figure 6.** X-ray crystal structures. Derivatives are shown in the SmSULT-OR crystal structure with solvent-accessible surfaces indicated. (A) Compound (*R*)-**9f** is shown as orange sticks. The solvent-accessible surface reveals two internal cavities into which additions to the OXA scaffold could be accommodated (red and blue ovals). (B) SmSULT-OR compound (*S*)-**11f**. (C) Electron density was calculated as a composite omit map<sup>35</sup> for the X-ray crystal structure of the (*S*)-**11f** complex (magenta) with SmSULT-OR. Compound (*S*)-**3** (OXA, yellow) from the complex with SmSULT-OR is overlaid for comparison (Protein Data Bank entry 5BYK<sup>36</sup>). Although the (*S*)-**11f** nitro group does not overlay the OXA position, the hydroxymethyl group matches the position observed with bound OXA (some atoms have been removed for clarity).

in an alternate location in the active site near R17 and N228. However, this orientation still places the hydroxymethyl moiety in a similar alignment to that observed for (*S*)-**3**, consistent with the proposed sulfotransferase mechanism. To clearly depict this observed difference, Figure 6C shows the crystal structure of the SmSULT-OR/compound (*S*)-**11f** complex (magenta) overlaid with the (*S*)-**3** (yellow)/SmSULT-OR complex.

We speculate that the alternate orientation for these two compounds occurs because the crystal structure contains the sulfate-depleted cosubstrate PAP where the absence of the sulfate enlarges the binding pocket. When the active cosubstrate 3'-phosphoadenosine-5'-phosphosulfate (PAPS) is bound, we expect the sulfate group will repel the alternate nitro position and the compounds will adopt the previously observed oxamniquine position. Additional observations in the crystal structures include a partially ordered (*S*)-**11f** molecule bound nonspecifically between sulfotransferase molecules at crystal packing interfaces and an oxidized M233 in the active site of the 3 complex structure. The nonspecific binding of compounds at the crystal packing interfaces appears to be an artifact caused by using a saturating concentration of the compounds to soak into the crystals. Oxidation of the methionine likely occurred with crystals stored at 22 °C over several weeks, while the protection from the reducing agent included in the protein preparation decreased over time.

As previously mentioned, the design and SAR of these analogs focused on manipulating the size and electronic nature of the *N*-benzyl substituent, along with a flexible amine core that allowed rotation of the benzyl moiety into the lipophilic pockets not occupied by **3**. Gratifyingly, the crystal structures of SmSULT-OR of analogs (*R*)-**9f** and (*S*)-**11f** provide evidence to support our design hypothesis focused on accessing the lipophilic regions (red and blue ovals in Figure 2B) not occupied by **3**.

In conclusion, a new chemical series of anti-schistosomal agents has been developed. Structure-based drug design guided by X-ray crystal structure analysis and SAR data from worm killing assays produced a number of novel small molecules with killing activity against *S. mansoni*, while a small number of analogs also showed varying levels of additional activity against *S. haematobium* and *S. japonicum*. To our knowledge, compound **12a** is the first example of an oxamniquine derivative active against all three species of *Schistosoma*. Our efforts are ongoing to find an analog that is more active against *S. haematobium* while maintaining drug-like

physicochemical properties. We will, in future reports, continue our exploration of the side chains and central core motifs and examine the SAR of the nitro group. Ideally, an anti-schistosomal agent will be obtained that can be used in combination therapy with **1** to prevent resistance.

## ■ ASSOCIATED CONTENT

### Supporting Information

The Supporting Information is available free of charge on the ACS Publications website at DOI: 10.1021/acsmchemlett.8b00257.

Experimental procedures and data for all new compounds synthesized, schistosomal assay description and additional *S. mansoni* data, X-ray structural data, molecular modeling and docking studies, and copies of 2D NMR spectra for compound **12a** (PDF)

## ■ AUTHOR INFORMATION

### Corresponding Authors

\*Tel: 210-458-8676. E-mail: stanton.mchardy@utsa.edu.

\*Tel: 210-567-3737. E-mail: loverde@uthscsa.edu.

### ORCID

Stanton F. McHardy: 0000-0003-0070-4924

### Author Contributions

These two Ph.D. student authors contributed equally to this work. The manuscript was written through contributions of all authors. All authors have given approval to the final version of the manuscript.

### Funding

The research was supported by a grant to P.T.L. and P.J.H. from the NIH, NIAID R01 AI115691. P.J.H. (AQ-1399) was funded by The Welch Foundation. The X-ray Crystallography Core Laboratory is a part of the Institutional Research Cores at the University of Texas Health Science Center at San Antonio (UT Health San Antonio) supported by the Office of the Vice President for Research and the Mays Cancer Center (NIH P30 CA054174). This work is based upon research conducted at the Northeastern Collaborative Access Team beamlines, which are funded by the National Institute of General Medical Sciences from the National Institutes of Health (P41 GM103403). This research used resources of the Advanced Photon Source, a U.S. Department of Energy (DOE) Office of Science User Facility operated for the DOE Office of Science by Argonne National Laboratory under Contract No. DE-AC02-06CH11357. Schistosoma material was provided by BRI via the NIAID schistosomiasis resource center under NIH-NIAID Contract No. HHSN272201000005I.

### Notes

The authors declare no competing financial interest.

### Biographies

Philip T. LoVerde received his Ph.D. in Epidemiologic Science from the University of Michigan under the direction of Profs. John Burch and Henry van der Schalie. His research interests are in host–parasite interactions, especially those that involve the human blood fluke, *Schistosoma*. His current research involves vaccine development, role of signal transduction in schistosome–host interactions, interplay between male and female parasites that results in female reproductive development, role of host genes in infection outcomes, genomics and genetic approach to identifying drug resistant genes, and a rational approach to novel drug development. He has published over 185 papers.

Stanton F. McHardy graduated from the University of Utah (Ph.D.) and served as a Pfizer Post-Doctoral Fellow with Professor Gary E. Keck. In 1996, Stan joined the Neuroscience group at Pfizer Global Research in Connecticut, focusing on Addiction, Schizophrenia, Cognition, and ADHD. Stan helped advance clinically investigated candidates in multiple programs and, as Associate Director, managed the CNS hit-to-lead efforts. In 2012, Stan became the Director of the Center for Innovative Drug Discovery (CIDD) at UT San Antonio. In the CIDD, Stan's collaborative programs focus on the discovery of small molecule therapeutics for a variety of disease areas.

## ABBREVIATIONS

OXA, oxamniquine;; N-Boc, *N*-tert-butylcarbamate; TBAF, tetrabutylammonium fluoride;; 1,2-DCE, 1,2-dichloroethane; DCM, dichloromethane; *S. m.*, *S. mansoni*; *S. h.*, *S. haematobium*; *S. j.*, *S. japonicum*; SmsULT-OR, *S. mansoni* sulfotransferase; ND, not determined.

## REFERENCES

- (1) King, C. H.; Dickman, K.; Tisch, D. J. Reassessment of the cost of chronic helminth infection: a meta-analysis of disability-related outcomes in endemic schistosomiasis. *Lancet* **2005**, *365*, 1561–1569.
- (2) Doenhoff, M. J.; Cioli, D.; Utzinger, J. Praziquantel: mechanisms of action, resistance and new derivatives for schistosomiasis. *Curr. Opin. Infect. Dis.* **2008**, *21*, 659–667.
- (3) Cioli, D.; Pica-Mattocchia, L.; Archer, S. AntiSchistosomal Drugs: Past, Present... and Future? *Pharmacol. Ther.* **1995**, *68*, 35–85.
- (4) Foster, R.; Cheetham, B. L. Studies with the schistosomicide oxamniquine (UK-4271) I. Activity in rodents and in vitro. *Trans. R. Soc. Trop. Med. Hyg.* **1973**, *67*, 674–684.
- (5) Valentim, C. L. L.; Cioli, D.; Chevalier, F. D.; Cao, X. H.; Taylor, A. B.; et al. Genetic and molecular basis of drug resistance and species-specific drug action in schistosome parasites. *Science* **2013**, *342*, 1385–1389.
- (6) Taylor, A. B.; Roberts, K. M.; Cao, X.; Clark, N. E.; Holloway, S. P.; Donati, E.; Polcaro, C. M.; Pica-Mattocchia, L.; Tarpley, R. S.; McHardy, S. F.; Cioli, D.; LoVerde, P. T.; Fitzpatrick, P. F.; Hart, P. J. Structural and enzymatic insights into species-specific resistance to schistosome parasite drug therapy. *J. Biol. Chem.* **2017**, *292*, 11154–11164.
- (7) Greenberg, R. M. New approaches for understanding mechanisms of drug resistance in schistosomes. *Parasitology* **2013**, *140*, 1534–1546.
- (8) Geary, T. G.; Sakanari, J.; Caffrey, C. R. Anthelmintic drug discovery: into the future. *J. Parasitol.* **2015**, *10*, 125–33.
- (9) Galdinoda Rocha Pitta, M.; Galdinoda Rocha Pitta, M.; de Melo Rêgo, M. J. B.; Galdino, S. L. The Evolution of Drugs on *Schistosoma* Treatment: Looking to the Past to Improve the Future. *Mini-Rev. Med. Chem.* **2013**, *13*, 493–508.
- (10) Rojo-Arreola, L.; Long, T.; Asarnow, D.; Suzuki, B. M.; Singh, R.; Caffrey, C. R. Chemical and genetic validation of the statin drug target to treat the helminth disease, schistosomiasis. *PLoS One* **2014**, *9*, e87594.
- (11) Fonseca, N. C.; da Cruz, L. F.; da Silva Villela, F.; do Nascimento Pereira, G. A.; de Siqueira-Neto, J. L.; Kellar, D.; et al. Synthesis of a Sugar-Based Thiosemicarbazone Series and Structure-Activity Relationship versus the Parasite Cysteine Proteases Rhodospain, Cruzain, and *Schistosoma mansoni* Cathepsin B1. *Antimicrob. Agents Chemother.* **2015**, *59*, 2666–2677.
- (12) Morel, M.; Vanderstraete, M.; Cailliau, K.; Lescuyer, A.; Lancelot, J.; Dissous, C. Compound library screening identified Akt/PKB kinase pathway inhibitors as potential key molecules for the development of new chemotherapeutics against schistosomiasis. *Int. J. Parasitol.: Drugs Drug Resist.* **2014**, *4*, 256–66.
- (13) Patel, G.; Roncal, N. E.; Lee, P. J.; Leed, S. E.; Erath, J.; Rodriguez, A.; et al. Repurposing human Aurora kinase inhibitors as leads for anti-protozoan drug discovery. *MedChemComm* **2014**, *5*, 655–658.
- (14) Long, T.; Neitz, R. J.; Beasley, R.; Kalyanaraman, C.; Suzuki, B. M.; Jacobson, M. P.; et al. Structure-Bioactivity Relationship for Benzimidazole Thiophene Inhibitors of Polo-Like Kinase 1 (PLK1), a

Potential Drug Target in *Schistosoma mansoni*. *PLoS Neglected Trop. Dis.* **2016**, *10*, e0004356.

- (15) Neves, B. J.; Andrade, C. H.; Cravo, P. V. Natural products as leads in schistosome drug discovery. *Molecules* **2015**, *20*, 1872–903.

- (16) da Silva, V. B. R.; Campos, B. R. K.; de Oliveira, J. F.; Decout, J.-L.; do Carmo Alves de Lima, M. Medicinal chemistry of antiSchistosomal drugs: Praziquantel and Oxamniquine. *Bioorg. Med. Chem.* **2017**, *25*, 3259–3277.

- (17) Pellegrino, J.; Pereira, L. H.; Mello, R. T.; Katz, N. Activity of Some Tetrahydro- and Pyrazinoquinolines against Early Developing Forms of *Schistosoma mansoni*. *J. Parasitol.* **1974**, *60*, 723–725.

- (18) Filho, R. P.; Souza Menezes, C. M.; Pinto, P. L. S.; Paula, G. A.; Brandt, C. A.; Silveira, M. A. B. Design, synthesis, and in vivo evaluation of oxamniquine methacrylate and acrylamide prodrugs. *Bioorg. Med. Chem.* **2007**, *15*, 1229–1236.

- (19) Filho, S. B.; Gargioni, C.; Silva Pinto, P. L.; Chiodelli, S. G.; Gurgel Velloso, S. A.; Silva, R. M. da; et al. Synthesis and evaluation of new oxamniquine derivatives. *Int. J. Pharm.* **2002**, *233*, 35–41.

- (20) Sadhu, P. S.; Kumar, S. N.; Chandrasekharam, M.; Pica-Mattocchia, L.; Cioli, D.; Rao, V. J. Synthesis of new praziquantel analogues: Potential candidates for the treatment of schistosomiasis. *P. S. Bioorg. Med. Chem. Lett.* **2012**, *22*, 1103–1106.

- (21) Kumar, S. N.; Sadhu, P. S.; Sharma, K. K.; Pica-Mattocchia, L.; Basso, A.; Cioli, D.; Rao, V. J. Synthesis and antischistosomal activity of new furoxan derivatives of praziquantel. *Indian J. Chem., SEC B* **2017**, *56B*, 112–119.

- (22) Hess, J.; Panic, G.; Patra, M.; Mastrobuoni, L.; Spingler, B.; Roy, S.; Keiser, J.; Gasser, G. *ACS Infect. Dis.* **2017**, *3*, 645–652.

- (23) Straathof, A. J. J.; Adlercreutz, P. *Applied Biocatalysis*; CRC Press, 2003.

- (24) Boehm, D.; Pryce, D. J. *Schistosoma haematobium*. *N. Engl. J. Med.* **2001**, *344*, 1170.

- (25) Lu, J. J.; Crimin, K.; Goodwin, J. T.; Crivori, P.; Orrenius, C.; Xing, L.; Tandler, P. J.; Vidmar, T. J.; Amore, B. M.; Wilson, A. G. E.; Stouten, P. F. W.; Burton, P. S. Influence of Molecular Flexibility and Polar Surface Area Metrics on Oral Bioavailability in the Rat. *J. Med. Chem.* **2004**, *47*, 6104–6107.

- (26) Lipinski, C. A.; Lombardo, F.; Dominy, B. W.; Feeney, P. J. Experimental and computational approaches to estimate solubility and permeability in drug discovery and development settings. *Adv. Drug Delivery Rev.* **2001**, *46*, 3–26.

- (27) Ackermann, J.; Bleicher, K.; Chomienne, O.; Mattei, P.; Sander, I. O. Novel Bicyclic Sulfonamide Derivatives Which Are L-CPT1 inhibitors. *US20100130484A1*, 2007.

- (28) Csatayova, K.; Davies, S. G.; Lee, J. A.; Ling, K. B.; Roberts, P. M.; Russell, A. J.; Thomson, J. E. Syntheses of trans-SCH-A and cis-SCH-A via a Stereodivergent Cyclopropanation Protocol. *Org. Lett.* **2010**, *12*, 3152–3155.

- (29) Ruiz-Castillo, P.; Buchwald, S. L. Applications of Palladium-Catalyzed C–N Cross-Coupling Reactions. *Chem. Rev.* **2016**, *116*, 12564–12649.

- (30) Jean, L.; Rouden, J.; Maddaluno, J.; Lasne, M. C. Palladium-Mediated Arylations of 3-Aminopiperidines and 3-Aminopyrrolidines. *J. Org. Chem.* **2004**, *69*, 8893–8902.

- (31) Evans, E. F.; Lewis, N. J.; Kapfer, I.; Macdonald, G.; Taylor, R. J. K. *N*-tert-Butoxycarbonyl (BOC) Deprotection Using Boron Trifluoride Etherate. *Synth. Commun.* **1997**, *27*, 1819–1825.

- (32) Gillis, E. P.; Eastman, K. J.; Hill, M. D.; Donnelly, D. J.; Meanwell, N. A. Applications of Fluorine in Medicinal Chemistry. *J. Med. Chem.* **2015**, *58*, 8315–8359.

- (33) Property calculations and data were archived and analyzed using the CDD Vault from Collaborative Drug Discovery (<https://www.collaborativedrug.com>). Within CDD Vault, ChemAxon's JChem Base was used for structure searching, chemical database access and management, and chemical property calculations. ChemAxon (<http://www.chemaxon.com>).

- (34) The evidence for preferentially binding and sulfur transfer of enantiomers of compound **3** was observed in previous work. See refs **5** and **6**.

(35) Terwilliger, T. C.; Grosse-Kunstleve, R. W.; Afonine, P. V.; Moriarty, N. W.; Adams, P. D.; Read, R. J.; Zwart, P. H.; Hung, L. W. Iterative-build OMIT maps: map improvement by iterative model building and refinement without model bias. *Acta Crystallogr., Sect. D: Biol. Crystallogr.* **2008**, *D64*, 515–524.

(36) Taylor, A. B.; Pica-Mattocchia, L.; Polcaro, C. M.; Donati, E.; Cao, X.; Basso, A.; Guidi, A.; Rugel, A. R.; Holloway, S. P.; Anderson, T. J.; Hart, P. J.; Cioli, D.; LoVerde, P. T. Structural and functional characterization of the enantiomers of the antiSchistosomal drug oxamniquine. *PLoS Neglected Trop. Dis.* **2015**, *9*, e0004132.